STUDIES OF FIBER -MATRIX ADHESION ON COMPRESSION STRENGTH[a]

W. D. BASCOM and J. A. NAIRN

University of Utah, Salt Lake City, Ut

D. J. BOLL

Hercules Aerospace, Inc., Magna, Ut

SUMMARY

A study has been initiated on the effect of the matrix polymer and the fiber-matrix bond strength on the compression strength of carbon fiber-polymer matrix composites. The work includes tests with micro-composites, single ply composites, laminates and multi-axial loaded cylinders. The results obtained thus far indicate that weak fiber-matrix adhesion dramatically reduces 0° compression strength. Evidence is also presented that the flaws in the carbon fiber that govern compression strength differ from those that determine fiber tensile strength. Examination of post-failure damage in the single ply tests indicates kink banding at the crack tip.

INTRODUCTION

In the development of advanced carbon fibers over the past decade, improvements in the compressive strength of carbon fiber reinforced polymer (CFRP) laminates has not kept pace with improvements in tensile strength. In Fig. 1, for example, there has been an increase of 40% in the tensile strength of Type II fibers with essentially no improvement in compression strength.

The increase in tensile strength has come about by decreasing the number and perhaps the type of flaws in the fiber through processing changes in the production of the polyacrylonitrile precursor and in the production of the carbon fiber itself. Obviously, these changes in the fiber microstructure have had no effect on compressive strength. In fact, the micromechanics of the compressive failure of CFRP is poorly understood. It is generally believed that failure occurs by a buckling of the fiber based on the observation of kink banding in post-failure examination (1,2). However, there is some evidence that the fibers fail in shear (3-5). Most of the theoretical work assumes fiber microbuckling (6,7) but the agreement between predicted and measured compressive strength is generally poor.

In the work reported here an effort is being made to identify the micromechanics of compressive failure with emphasis on the effect of the polymer matrix and the bond strength between matrix and fiber. The experimental approach is to examine compressive failure at several levels of test specimen complexity; microcomposites of 1 to 5 fibers embedded in matrix polymers, embedded single ply specimens, unidirectional laminates and finally multiaxially loaded cylinders. Work with the cylinders is not scheduled to begin until April 1991.

MATERIALS

Batches of carbon fiber taken from specific production lots were procured from Hercules (Hercules Aerospace, Magna UT) and set aside for all of the tests in this study. The fibers include sized and G-sized AS4, IM7, and HMS4. The G-sizing is a commercial epoxy compatible sizing. In addition, AS4 and IM7 fibers were coated with a release agent (Frecote 700) and given the designation AS4F and IM7F.

Samples of these fibers were analyzed for surface chemical composition using x-ray photoelectron spectroscopy. The results are listed in Tables I and II. The percent elemental composition for the unsized and G-sized fibers are consistent with published data (8,9). Note the high silicon content on the AS4F and IM7F fibers (Table I) and that the silicon is present as an organo-silicon moiety, i.e., -Si-O-C- (Table II). These results indicate that the release coating is a polysiloxane. Depth profiling of the F-coating using Auger spectroscopy indicated that the coating is approximately 25nm thick and uniformly distributed.

The embedding resins used in the microcomposite and single ply experiments were two diglycidylether Bisphenol A epoxides (DGEBA, Dow DER 332 and Shell Epon 828) cured with either m-phenylene diamine (m-PDA), a polyamine (Texaco D230) or a proprietary amine (Dow DEH 24). An accelerator (AC399) was used with the polyamine curative.

MICROCOMPOSITES

Test Methods

In these experiments the test specimen consists of a single filament embedded lengthwise through the center of a block of transparent epoxy (DGEBA + m-PDA) measuring 3cm x .95cm x .35cm (1.19in. x 0.375in. x 0.125in). The specimen is placed in a compression test fixture fitted with a piezoelectric stress transducer. The specimen is held by side supporting key ways with a clearance of about 1.2×10^{-2}mm (0.005in.). The load is applied hydraulically through an actuator which transmits the force through the load cell and then to a steel bar in contact with the specimen. The space between the side supports permits viewing the fiber using transmitted light with crossed polarizing filters.

The test fixture was mounted on an optical bench as shown in Fig. 2.

478

Further details of this test procedure can be found in reference 5.

Tensile tests were also done on embedded single filament specimens to determine the fiber-matrix bond strength. Details of this technique can be found in reference 10. Briefly, the specimen, in the form of a miniature dogbone, is placed in a tensile test fixture on the stage of a transmitted light microscope. The test fixture is fitted with an LVDT to measure strain. As the specimen is loaded, the filament fragments until reaching a critical fragment length, l_c, which can be related to the fiber-matrix boundary strength. Ancillary information about the interphase or interfacial strength is obtained from the stress birefringence patterns at fiber breaks when the specimen is viewed between crossed polarizing filters.

Results: Single Filament Compression Tests

In an effort to determine the onset load for fiber fragmentation, the load was applied incrementally at 100 lb. increments. Initial tests indicated that there is a short delay in the development of fiber breaks at a given load so the load was held constant for 3min before counting the number of breaks. Tests were conducted on AS4, AS4G, IM7G and AS4F and the results are presented in Fig. 3.

For the AS4, AS4G and IM7G fibers the majority of fragmentation occurs between 15-20 ksi (103-138 MPa) beyond which the number of breaks increases by only 10 -20% up to the maximum load of 30 to 35ksi (210-240 MPa). Some of the breakage at the higher loads may be due to yielding of the matrix. We are presently determining the load at which yielding (permanent deformation of the specimen) begins. Each datum point in Fig. 3 is an average from 3-4 specimens.

The fact that the onset of extensive fragmentation occurs over the same load range for all three fibers, suggests that they have essentially the same compression strength. As discussed later the 0° laminate strengths for these fibers are reported to be essentially the same. It is instructive to compute the stress in the fiber at the fragmentation loads in Fig. 3 which can be obtained by multiplying the fragmentation stress by the ratio of the fiber modulus to the matrix modulus; E_f/E_m = 90. The majority of the fragmentation took place between 12-20ksi (827-138MPa) so the failure strains of the fibers are of the order of 1080-3150ksi (74.4-283 GPa). These values are more than 4x the compression strength of a 0° laminate. However, it is doubtful that the full compressive strength of the fiber is realized in laminate testing. On the other hand, whether the fiber failure strains calculated here are realistic is highly problematical.

It is not obvious why the IM7G fiber developed 3X the number of breaks than the AS4 or AS4G. This result would suggest a higher population of flaws in the IM7 fiber compared to AS4. However, we cannot rule out some mechanical aberration of the test condition. For example, stress transfer may be more efficient into the higher modulus IM7 fiber. Also, the tensile modulus of IM7 is about 20% greater than AS4 so that for a given load on the specimen the strain in the IM7 fiber is approximately 20% greater.

The results for the AS4F fiber are also presented in Fig. 3. This fiber had been sized with a release agent in order to reduce fiber-matrix adhesion. Results are presented below that the coating did essentially eliminate adhesion. The embedded AS4F exhibited a very low level of fragmentation that increased more or less linearly with increasing load. It would appear that the low adhesion significantly reduced the transfer of compression stress from the matrix into the fiber.

Results: Single Filament Tensile Tests

The fiber-matrix adhesion strength can be determined using the single embedded filament tensile test. When the fiber fragment length reaches the critical length, i.e., the fragment is too short for stress transfer to reach the fiber tensile strength, σ_c. The boundary shear strength, τ, is given by

$$\tau = \frac{\sigma_c d_f}{2 l_c} \qquad [1]$$

where d_f is the fiber diameter and l_c is the critical length. A number of assumptions are needed to transform the experimental critical length data into boundary shear strengths, the most difficult being how to express the statistical distribution of the fiber tensile strength. Some of this uncertainty can be avoided by simply taking the critical aspect ratio, l_c/d_f as a *relative* measure of interfacial strength. This approach requires that comparisons be made for fibers that have similar tensile strengths and strength distribution. This assumption is not entirely valid for the fibers tested here. None the less, for present purposes the comparison of critical aspect ratios is a useful approximation.

The critical aspect ratios for the AS4 and IM7 fibers are listed in Table III. The matrix was DGEBA (Epon 828) cured with m-PDA. Each datum point is the average of 10-12 specimens. The observed values are comparable to values published elsewhere (10). They are in the range expected for strong adhesion and this conclusion was supported by the stress birefringence observations.

No fiber breaks were observed for the AS4F fiber in the same epoxy up to a nominal strain level of over 4.6%. Evidently, the critical length is greater than the length of the embedded filament, 2.5cm, and so the critical aspect ratio is greater than 3751! Clearly, the release coating on this fiber has essentially eliminated any adhesion both frictional as well as chemical.

In these tests the fragmentation "rate" was measured and plotted as breaks/mm *vs* applied strain. The results are presented in Figs. 4-7. There was a more or less linear increase in the fragmentation up to the critical length. Note that this initial slope is lower for the AS4G compared to the unsized AS4 and dramatically reduced in the case of IM7G compared to IM7. The lower slopes for the sized fibers indicate fewer weak flaws. Evidently, the sizing does protect the fiber from damage during spooling and packaging. Flaws produced during processing are usually severe surface flaws.

SINGLE PLY COMPRESSION TESTS

Test Methods

Our goal in single ply compression experiments is to develop a test procedure by which we can directly measure the compression strength of single plies and can also observe the initiation and propagation of compression damage during the experiments. The testing jig is shown in Fig. 8. In brief, the sample is sandwiched between two constraining plates. The plates are coated with grease or a similar non-stick substance to minimize the loads transferred into the sample sides through friction. The compressive load is applied uniaxially using shim stock whose thickness is matched to the single-ply specimen. The front constraining plate is made of transparent Lucite to allow observation of the samples during testing.

Our first experiments were with rectangular shaped single ply graphite/polysulfone composites. These failed at the sample ends by a crushing mechanism. To minimize end-effects we adopted the mini-dogbone geometry shown in Fig. 8. Single-ply mini-dogbone specimens failed by longitudinal splitting or by out-of plane buckling. These types of failures are not representative of uniaxial compression failure. To get uniaxial compression failures we added extra constraint to the single-ply specimens by embedding them in an epoxy. By using the lateral side supports shown in Fig. 8 in addition to an embedding epoxy, we were able to minimize the amount of embedding epoxy required to get compressive failures. The less embedding epoxy used, the less we need to correct our measurements to determine composite compression strength.

To determine the amount of embedding epoxy required, we measured the load at failure as a function of total specimen thickness. In each sample, the single-ply was 5 mils thick and located approximately at the center of the specimen and the amount of embedding epoxy was varied to vary the total sample thickness. The measured load at failure was converted to the compression of the composite using a simple rule-of mixtures formula:

$$\sigma_c = \frac{P_{total}E_c}{(E_cA_c + E_eA_e)}$$

where E_c and E_e are the moduli of the composite single ply and of the embedding epoxy and A_c and A_e are the cross-sectional areas of the composite single ply and of the embedding epoxy at the location of the compression failure.

Experimental results for a graphite/polysulfone matrix single-ply composite are presented in Fig. 9. The 5 mil samples are for unembedded single plies and they fail at a very low loads. As the thickness of the embedding epoxy is increased, the failure load increases and appears to reach a plateau value for samples with thicknesses above 24 mils. Observation of the failures also suggests that the thicker samples fail by an in-plane axial compression failure mode while the thinner samples exhibit significant out-of plane buckling. The average compressive stress of the 24 mil and thicker

specimens was 810 MPa. This result is close to 0° compression strength literature values for graphite/polysulfone laminates (800-1000 GPa).

Similar tests of AS4/3501 single-ply composites gave similar results. The compression strength increased and reached a plateau for specimens thicker than 19 mils. The average compression strength for the samples thicker than 19 mils was 1470 MPa. This result is close to the literature value of 1600 to 1700 MPa for 0° compression strength.

The amount of embedding epoxy required to achieve in-plane compression failure is about 3-4 times the thickness of the single ply. By measuring the compression properties of neat embedding epoxy, it was determined that in these specimens, about 80% of the load is carried by the composite and therefore the amount of correction required to extract the composite compression strength is small. We also note that the compression failure, which is always at the middle of the sample, begins at one edge and propagates towards the middle. The crack propagates across the sample in about 1 second.

A specimen preparation procedure has been developed that addresses two critical problems: minimizing bubble formation in the embedding resin and alignment of the ply so that it is centered and parallel to the loading direction. Sample misalignment within the embedding epoxy will introduce scatter in the experimental results. The single-ply specimens are cured in a mold under pressure in a hot press. If pressure is applied too soon after start of cure, the embedding epoxy viscosity is too low and the pressure causes movement of the single ply resulting in poor alignment. To avoid this problem, pressure is not applied until 10 to 15 minutes after the start of cure. During this waiting time the viscosity of the epoxy increases (as observed by a parallel batch of neat epoxy). When pressure is applied to the higher viscosity curing epoxy there is much less movement of the ply. Alignment can easily be checked visually by observing the specimen edge-on which is routinely done for all specimens.

The number of entrapped bubbles was minimized by out-gassing the epoxy before specimen preparation.

Results

Single-ply compression tests have been done on the following fiber types — AS4, AS4G, IM7, IM7G and HMS4. Each of these fibers was prepregged with Hercules 3501-6 epoxy. The embedding epoxy consisted of a DGEBA epoxide (DER332) a curative (D230) and an accelerator (AC399). The results are presented in Table IV. Each reported number is an average of at least 20 measurements.

There is some dependence of the compression strength on the fiber type with the AS4 fibers giving the highest compression strength, IM7 fibers giving a slightly lower compression strength, and HMS4 fibers giving a significantly lower compression strength. The difference between the AS4 and IM7 results may not be statistically significant. In addition to the observed strength differences there were differences in the mode of failure. The AS4

and the IM7 plies fail suddenly; in other words, immediately after crack initiation, the damage propagates through the entire cross section of the specimen. In contrast, the HMS4 plies fail by slow crack growth. With HMS4 plies, it is possible to stop the test and arrest the damage process.

There was no significant effect of the G sizing. The AS4 fibers showed no effect and the result for the IM7G fiber was 7% lower than for the unsized fiber. This 7% difference is probably within experimental error.

An anticipated advantage of the single ply tests is the ability to observe failures as they occur. Samples of AS4/3501-6 and IM7/3501-6 tested at relatively high cross-head rates (0.1 mm/sec) exhibited two types of failure - rapid unstable failure across the entire composite cross section and slow stable compression failure propagation. The stable crack growth was nearly always associated with flaws in the embedding epoxy, notably trapped air bubbles.

Post-failure analyses have been done on the single-ply compression samples where the crack had arrested within the ply. The samples were potted in a clear epoxy, sectioned through the compression damage as shown in Fig. 2, polished, and examined using light microscopy. Two types of damage were observed as shown in Fig. 10. The side of the section cut near the crack tip revealed a distinct kink band (Fig. 10A). The other side of the section which was about 2.5cm (0.1in.) back from the crack tip revealed a complex damage pattern that included kink banding, longitudinal splitting and planes of shear failure (Fig. 10B). Presumably, some of this damage was the result of post-failure crushing.

An obvious concern is that the embedding epoxy should only provide support and not influence the compression strengths measured for the single plies. To test for this effect we tested specimens that were identical except for the embedding epoxy. The most important property of the epoxy is probably its modulus and we therefore varied the embedding epoxy modulus.

We used two different epoxys; Epoxy 1 (DER332 + D230 + AC399) which has a compression modulus of 2.85 GPa and Epoxy 2 (DER 332 + DEH24) which has a compression modulus of 2.25 GPa. Thus, Epoxy 2 has a compression modulus that is 21% lower than that of Epoxy 1. The compression moduli of these two epoxies were measured on specimens prepared identically to the single-ply compression specimens except lacking the single ply. We used these epoxies to embed IM7/3501-6 and HMS4/3501-6 single plies. The specimens were tested in compression and the results are presented in Table V; each reported number is an average of at least 20 specimens.

The compression strengths in Epoxy 2 are 2% to 8% lower than those in Epoxy 1. These differences are small and within experimental uncertainty. We suggest that for embedding epoxys with compression moduli greater or equal to those used here (≥ 2.25 GPa) that the observed compression strengths and compression properties of embedded single plies are independent of the properties of the embedding epoxy. It is possible that much lower moduli embedding epoxies would not provide sufficient support and therefore might affect the results.

LAMINATE TESTING

0° Compression Tests

Tests have been completed for AS4, AS4G, AS4F, IM7, IM7G, IM7F, HMS4, HMS4G and HMS4F fibers in 3501-6. The results are presented in Table VI. The AS4 and the IM7 laminates have essentially the same compression strength for both unsized and G-sized fiber. The HMS4 laminates, unsized and G-sized, had compression strengths of one-half of that obtained for the AS4 and IM7.

Sizing the fiber with a release coating reduced the compression strength of the AS4 and IM7 laminates by nearly a factor of three. The effect of the release coating on the HMS4 compression strength was less than 25%.

Clearly, a reduction in the fiber-matrix adhesion significantly reduces the 0° compression strength. The fact that the compression strength of the HMS4 laminates was significantly less than for the AS4 and IM7 laminates and that applying a release coating to the HMS4 fiber had less of an effect than for the AS4 or IM7 suggests that the adhesion between the HMS4 and the 3501-6 matrix is inherently low. This conclusion is supported by adhesion measurements using the single embedded filament test (11,12) and from short beam shear tests (13). The low adhesion of the HMS4 has been attributed to a cohesively weak skin of highly oriented graphite basal planes that have low resistance to interfacial shear stresses. Application of the release coating to the HMS4 fiber reduces the adhesion even further and probably shifts the interfacial failure from the fiber skin to the fiber-matrix interface.

GENERAL DISCUSSION

The results of the single filament microcomposite compression tests indicate that failure occurs as a sudden avalanche of fiber breaks over a relatively narrow stress range. This behavior is distinctly different than the fragmentation of single filament microcomposites tested in tension where fragmentation is progressive with increasing load. This difference in behavior indicates different types of fiber flaws are involved in compression failure compared to tensile failure.

Application of a polysiloxane release coating to the AS4 and IM7 fibers essentially eliminated any bonding between fibers and matrix. In microcomposite compression testing of the IM7F fiber, the rate of fragmentation was significantly reduced indicating that, because of the loss in adhesion, there was little capability for stress transfer from the matrix into the fiber.

A single ply compression test technique has been developed. When failure is confined to in-plane crack propagation across the ply, the measured compression strengths were comparable to the 0° laminate compression strengths.

In the single ply tests and the 0° laminate tests of the HMS4/3501-6, the

484

compression strengths were significantly lower compared to the compression strengths of AS4/3501-6 and IM7/3501-6. The low strengths of this high modulus fiber is attributed to low fiber-matrix adhesion (12,13).

The G-size had no discernable effect on compression strength in the single ply and 0^0 laminate tests. However, the application of a release coating on the AS4 and IM7 fibers reduced the 0^0 laminate compression strength by a factor of three. The effect of the release coating on the HMS4 fiber resulted in only a 25% reduction in compression strength which suggests that the release coating made an inherently weak interface only slightly worse.

CONCLUSIONS

Single filament microcomposite tests indicated that the fiber flaws responsible for compression failure are different from the fiber flaws that control tensile failure.

The single filament microcomposite tests, the single ply composite tests and the 0^0 laminate tests all indicate that the compression strength of AS4 and IM7 are essentially identical. The HMS4 single ply and laminate tests resulted in a much lower compression strength than the other fibers due to low fiber-matrix adhesion.

Applying a polysiloxane release coating to the AS4 and IM7 fibers effectively eliminated any adhesion between fiber and matrix. As a result, there was very little stress transfer from the matrix into the fiber and the laminate compression strengths were reduced by a factor of three compared to the unsized and G-sized fibers.

It should be kept in mind that this paper represents "work in progress". The results and conclusions presented here should be viewed as tentative and subject to revision as the study progresses.

REFERENCES

1. Parry, T. V. and Wronski, A. S., "Kinking and Tensile Compression and Interlaminar Shear Failure Mechanisms in CFRP Beams Tested in Flexure," J. Mat. Sci., 16 439 (1981)

2. Hahn, H. T. and Williams, J. G., Mechanics of Composites Review, Dayton OH, Oct. 1984, p.121

3. Ewins, P. D., and Potter, R. T., Phil. Trans. Roy. Soc., A295 507 (1980)

4. Hawthorne, H. M. and Teghtsoonian, E., J. Mat Sci., 10 41 (1975)

5. Boll, D. J., Jensen, R. M., Cordner, L. and Bascom, W.D., "Compression Behavior of Single Carbon Filaments Embedded in an Epoxy Polymer," J. Comp. Mat., 24 209 (1990)

6. Rosen, V. M., "Mechanics of Composite Stengthening in Fiber Composite Materials", ASM, 1965, p37

7. Hahn, H. T. and Williams, J. G., "Composite Failure Mechanisms in Unidirectional Composites, NASA Tech. Memo, 85835, Aug, 1984

8. Procter, A. and Sherwood, P. M. A., "X-ray Photoelectron Spectroscopic Studies of Carbon Fibre Surfaces. I. Carbon Fibre Spectra and the Effects of Heat Treatment," J. Electron Spectroscopy and Related Phenomena, 27 39 (1982)

9.Takahagi, T. and Ishitani, A., "XPS Studies by use of the Digital Difference Spectrum Technique of Functional Groups on the Surface of Carbon Fiber," Carbon 22 43 (1984)

10.W. D. Bascom and R. M. Jensen,"Stress Transfer in Single Fiber/Resin Tensile Tests," J. Adhesion, 19 219 (1986)

11. Drzal, L. T.; Rich, M.J.; and Lloyd, P.F.; "Adhesion of Graphite Fibers to Epoxy Matrices; I, The Role of Fiber Surface Treatment, "J. Adhesion, 16 1 (1983)

12. Dilandro, L. DiBenedetto, A. T. and Groeger, J., "The Effect of Fiber-Matrix Stress Transfer on the Strength of Fiber-Reinforced Composite Materials," Polymer Composites 9 209 (1988)

13. Hercules Carbon Fiber Product Data Sheets, Hercules Inc. Hercules Plaza, Wilmington DE 19895

TABLE I

ELEMENTAL SURFACE ANALYSIS CARBON FIBERS

(Atomic Elemental %)

Fiber Type	C	O	N	Si	Na	Cl	F	Ca
AS4/12K	84	9.1	4.8	0.4	1.0	0.0	0.0	0.0
AS4G/12K	82	14	2.5	0.7	0.6	0.3	0.0	0.0
AS4F/12K	52	26	1.1	21	0.0	0.0	0.0	0.0
IM7/12K	82	13	4.3	0.4	0.1	0.0	0.0	0.0
IM7G/12K	84	13	3.1	0.0	0.1	0.0	0.0	0.2
IM7F/12K	56	26	2.3	17	0.0	0.0	0.0	0.0
HMS4/12K	93	5.1	0.0	0.3	1.4	0.1	0.0	0.0
HMS4G/12K	88	10	0.0	0.0	1.6	0.0	0.0	0.0
HMS4F/12k	59	22	0.0	18	0.0	0.0	0.0	0.0

G in the fiber type is for "G" sizing
F in the fiber type is for FreKote size

TABLE II

HIGH RESOLUTION ESCA FOR CARBON AND SILICON

Atomic Elemental %*

Fiber Type	C_1	C2	C_3	S_1	S_2
AS4/12K	64	14	6.3	0.2	0.2
AS4G/12K	61	21	0.0	0.2	0.5
AS4F/12K	50	2.9	0.0	21	0.0
IM7/12K	62	13	6.4	0.4	0.0
IM7F/12K	49	5.6	0.9	17	0.0
HMS4/12K	80	13	0.0	0.3	0.0
HMS4F/12K	58	1.0	0.0	18	0.0

*Where C_1 = C-R or R-CH
C_2 = C-OR
C_3 = O-C-OR
S_1 = Organic silicone
S_2 = SiO_2

Table III
Critical Aspect Ratios for the AS4 and IM7 Fibers

Fiber	Critical Aspect Ratio	Standard Deviation
AS4	46	6
AS4G	52	8
IM7	66	9
IM7G	66	4

Table IV
Single-ply Compression Strengths

Fiber Type	Compression Strength (GPa)
AS4	1.42
AS4G	1.43
IM7	1.39
IM7G	1.29
HMS4	0.73

Table V
The Compressions Strengths of IM7G/3501-6 and HMS4/3501-6
Single Plies Embedded in Epoxys having Different Moduli.

Fiber Type	σ_c in Epoxy 1 (GPa)	σ_c in Epoxy 2 (GPa)	$\dfrac{\sigma_c \text{ in Epoxy 2}}{\sigma_c \text{ in Epoxy 1}}$
IM7G	1.31	1.29	0.98
HMS4	0.73	0.67	0.92

Table VI
0° Compression Strengths

	Unsized		G sized		Release coat sized	
Fiber Type	Mean GPa/ksi	Std. Dev. GPa/ksi	Mean GPa/ksi	Std. Dev. GPa/ksi	Mean GPa/ksi	Std. Dev. GPa/ksi
AS4	1.97/285	.149/21.6	1.92/279	.108/15.6	.724/105	.08/11.8
IM7	2.05/296	.095/13.8	2.08/302	.103/14.9	.869/126	.10/14.9
HMS4	1.03/149	.058/8.4	1.00/145	.038/5.5	.786/115	.08/11.9
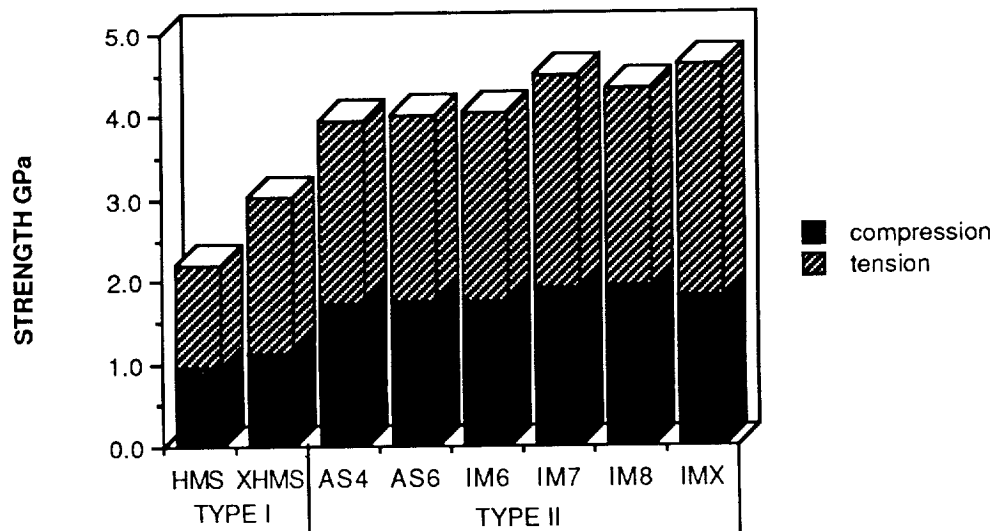
Figure 1 - Uniaxial laminate compression strength *vs* tensile strength (Hercules 3501-6 matrix)
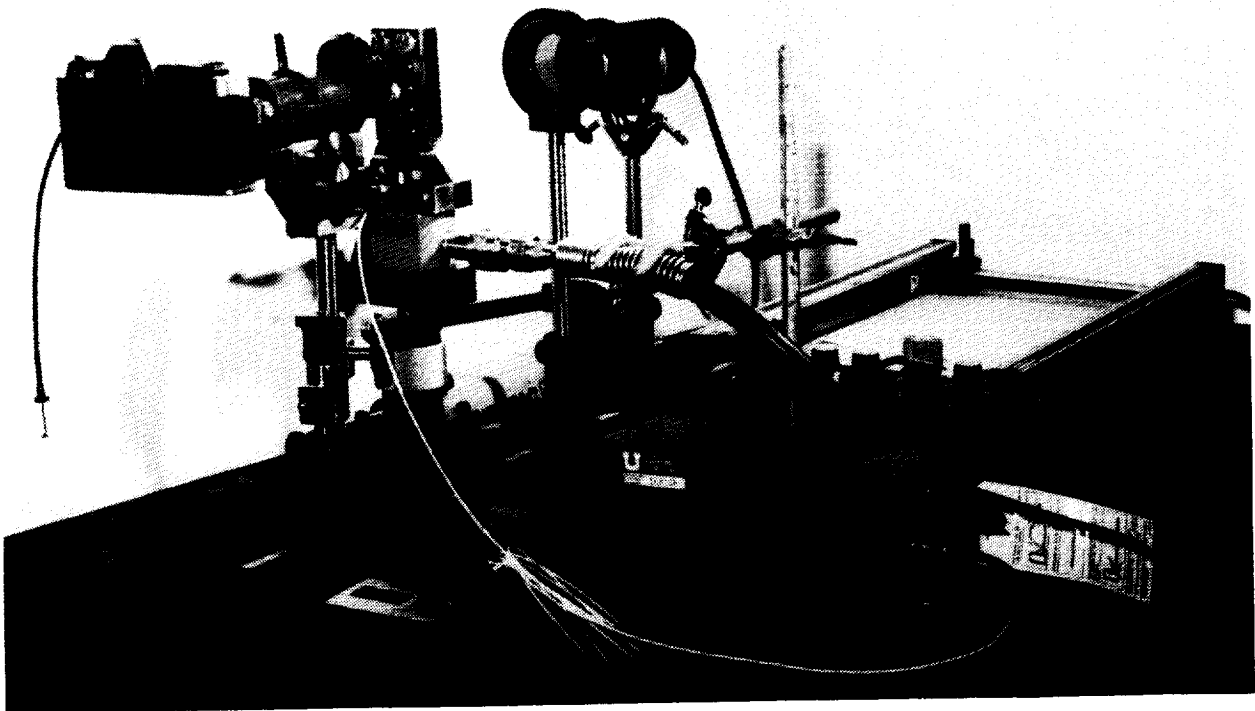
Figure 2 - Optical bench with test fixture for microcomposite compression studies
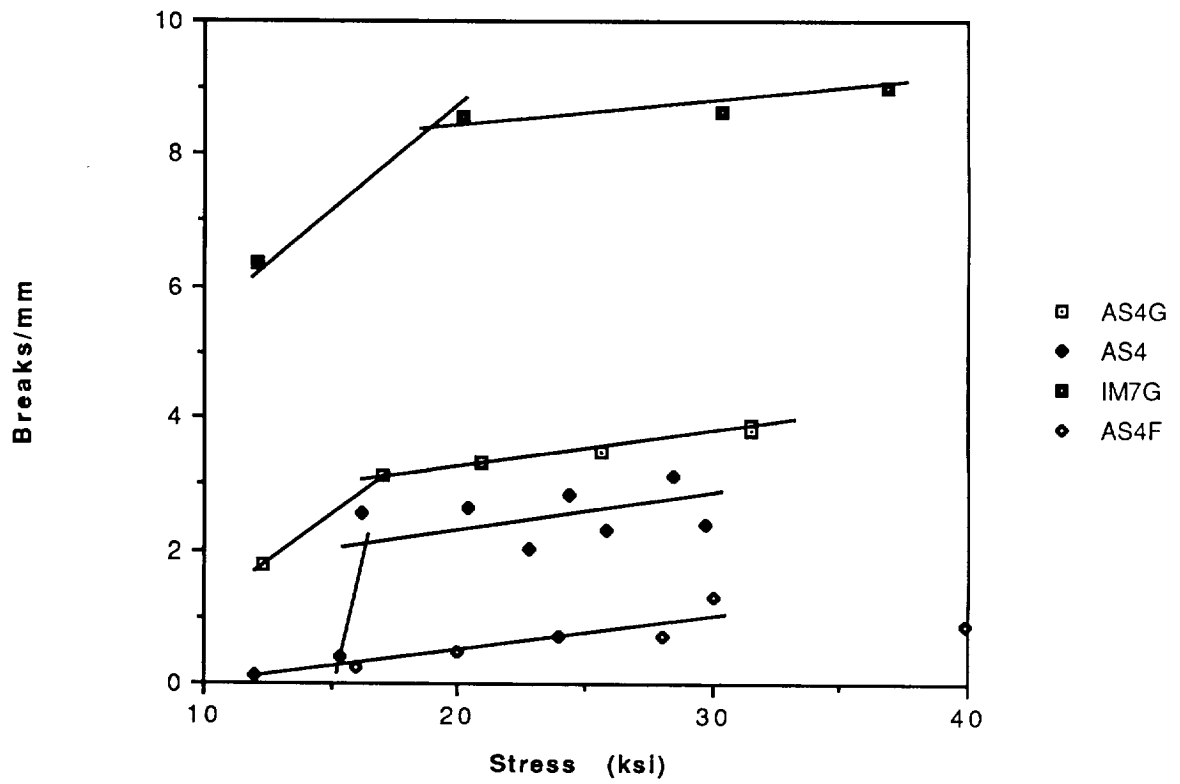
Figure 3 - Fiber fragmentation with increasing stress for single embedded filament compression tests.
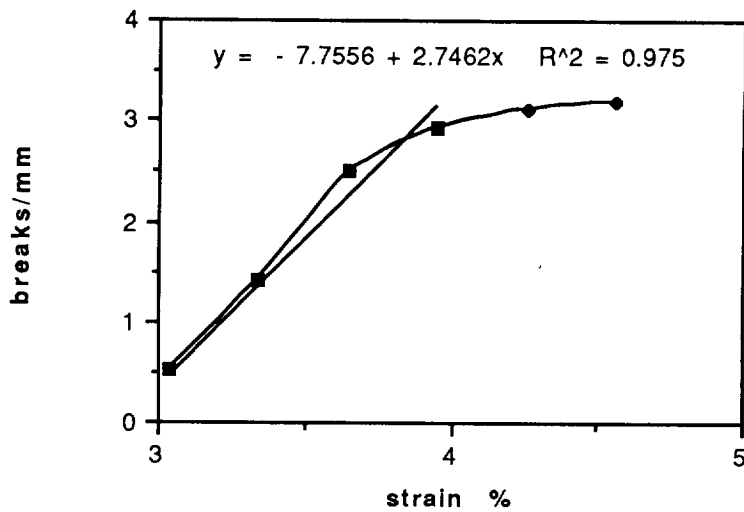
Figure 4 - Fragmentation of AS4 fiber in tension

491
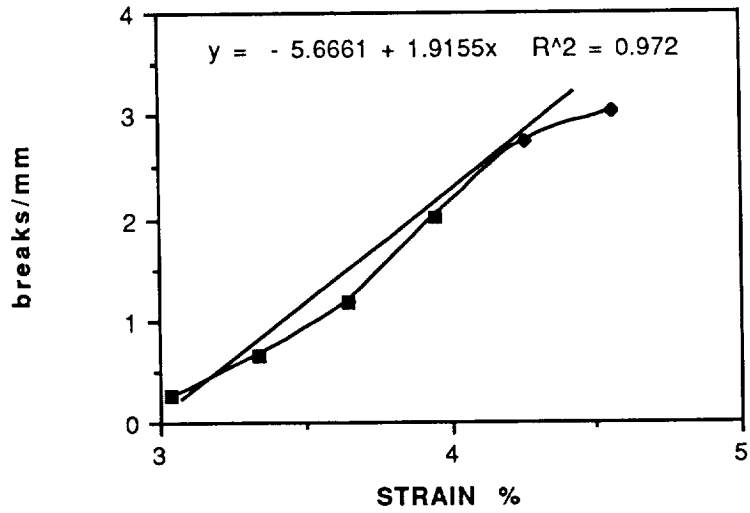
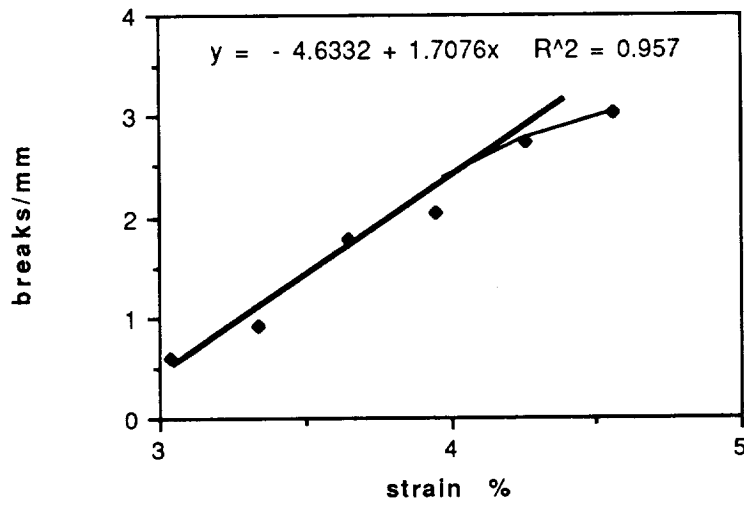Figure 5 - Fragmentation of the AS4G fiberin tension.
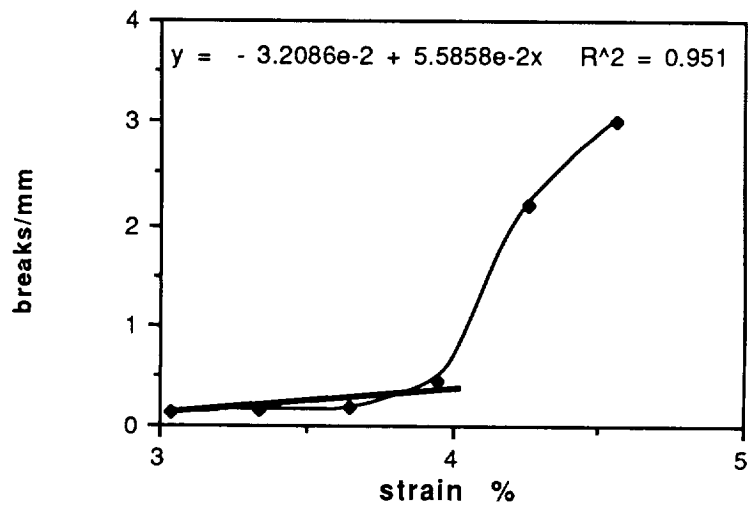

Figure 6 - Fragmentation of the IM7 fiber in tension.
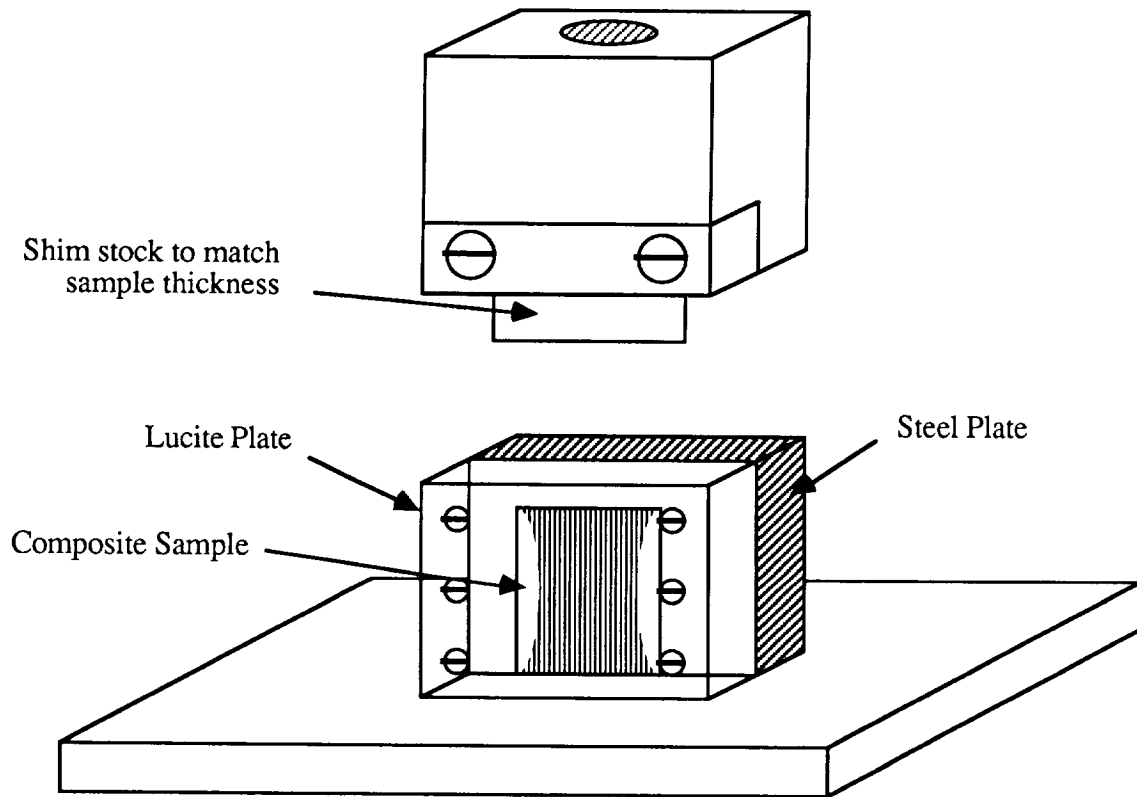
Figure 7 - Fragmentation of the IM7G fiber.

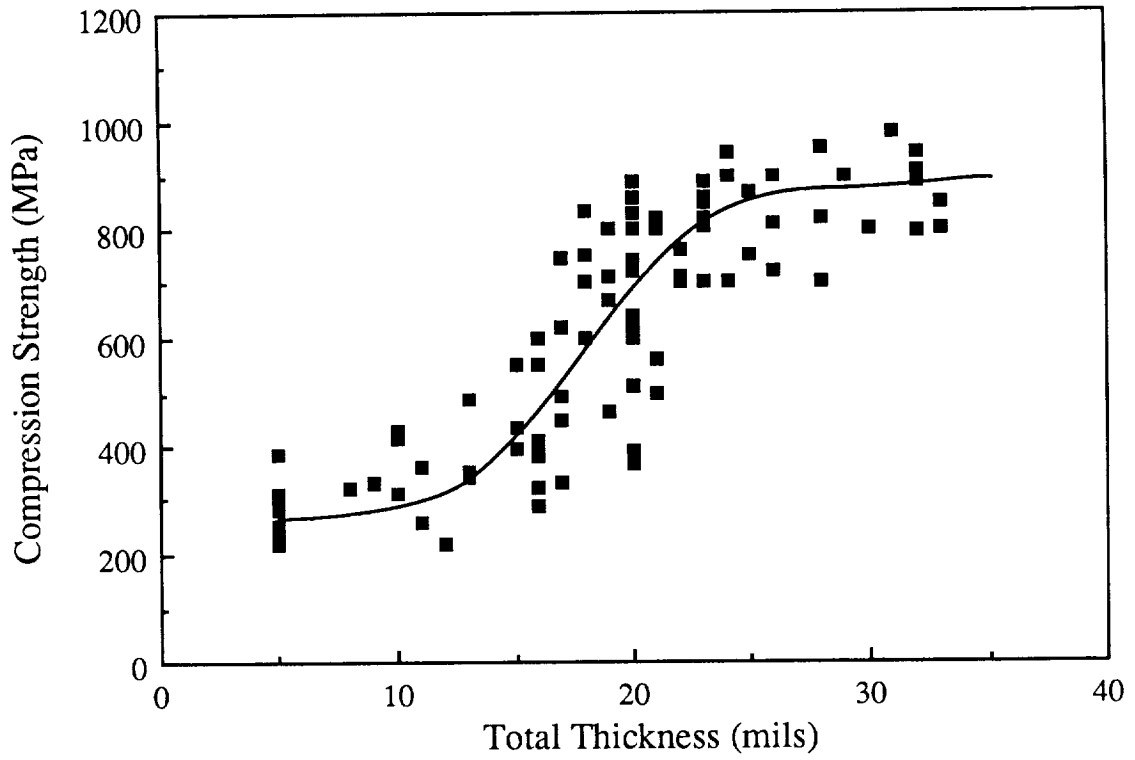Figure 8 - Test configuration used to obtain compression failures of single-ply composites.

Figure 9 - The compression strength of single-ply graphite/polysulfone composites as a function of total sample thickness.

$$\overline{0.1\text{mm}}$$

Figure 10 - Damage observed at a crack tip (A) and 2.5cm behind the crack tip(B) for a single ply compression crack.